



Communication

Promoting condensation kinetics of polymeric carbon nitride for enhanced photocatalytic activities



Dongya Ni, Yuye Zhang*, Yanfei Shen, Songqin Liu, Yuanjian Zhang*

Jiangsu Engineering Laboratory of Smart Carbon-Rich Materials and Device, Jiangsu Province Hi-Tech Key Laboratory for Bio-Medical Research, School of Chemistry and Chemical Engineering, Medical School, Southeast University, Nanjing 211189, China

ARTICLE INFO

Article history:

Received 5 March 2019

Received in revised form 10 April 2019

Accepted 29 April 2019

Available online 29 April 2019

Keywords:

Polymeric carbon nitride

Condensation kinetics

Fast ramping rate

High crystallinity

Photocatalytic hydrogen evolution

ABSTRACT

Polymeric carbon nitride (CN) semiconductor by thermal condensation of N-rich precursors has attracted much attention for its capability ranging from photocatalytic and photoelectrochemical energy conversion to biosensing. However, the influence of condensation process on the final structure of CN was rarely studied, making the condensation kinetic far from being fully optimized. Herein, we report the preparation of CN by a simple condensation kinetics modulation using a faster ramping rate during the polymerization process. The modified condensation recipe was even simpler than the conventional one, but led to an improved photocatalytic H₂ evolution up to 3 times without any additional chemicals or other complements. Detailed mechanism studies revealed the increase of crystallinity and surface area due to the rapid condensation played the key roles. This work would offer a more facile and effective way to prepare bulk CN for large-scale industrial applications of bulk CN with higher photocatalytic activities for sustainable energy, environmental and biosensing.

© 2019 Chinese Chemical Society and Institute of Materia Medica, Chinese Academy of Medical Sciences. Published by Elsevier B.V. All rights reserved.

Due to continuing energy crisis and deteriorative environmental problems from fossil fuel, renewable solar energy is considered a promising alternative to address these global issues [1,2]. The exploration of highly efficient and noble metal-free photocatalysts for the conversion of solar energy to chemical energy has been widely investigating, especially photocatalytic water splitting to produce hydrogen, which has a high energy content (120–142 MJ/kg) [3–6]. As a metal-free photocatalyst, polymeric carbon nitride has attracted much attention for its capability of water splitting under visible light irradiation which was firstly reported in 2009 [7]. Moreover, CN exhibits many extraordinary features, such as environmental friendliness, earth-abundant resource, high thermal and chemical stability, and interesting optical and electronic properties [8–12]. However, bulk CN generally suffers from low specific surface area, low absorbance in visible light, high charge-carriers recombination rate and low crystallinity, which limits its potential applications in photocatalytic water splitting [13–15], photocatalytic CO₂ reduction [16–18], organic pollutants degradation [19,20], and other emerging optical applications, such as photoluminescent (PL) and electrochemiluminescent (ECL)

biosensing [21–23]. To solve these problems, various strategies have been developed to improve the photocatalytic performance of CN, including engineering the chemical, optical or electronic structure and other properties of CN photocatalysts [24–28]. For example, it is extensively used that utilization of chemical doping to tailor the electronic structure of CN [29,30], template-assisting preparation method to design CN nanostructures and morphology [31,32], heterojunction construction to promote photogenerated electron-hole pairs separation [33–36], and precursor preorganization to make functional group modification [37].

An alternative approach is to improve the crystallinity of CN, which is supposed to promote the kinetics of charge-carriers diffusion in both the bulk and the surface in principle, but the related studies are still in infancy. Only a few examples are reported in previous work, for instance, Li and co-workers prepared condensed carbon nitride nanorods with improved crystallinity by using the confined thermal condensation of cyanamide inside the channels of anodic aluminum oxide templates [38]. In another interesting work, Guo *et al.* reported the synthesis of high crystalline CN with decreased structural imperfections by judiciously combining the implementation of melamine-cyanuric acid (MCA) supramolecular aggregates and microwave-assisted thermal polymerization [39]. We recently successfully tailored the crystallinity of bulk CN by engineering the hydrogen-bonding interactions *via* introducing a simple

* Corresponding authors.

E-mail addresses: zhangyuye@seu.edu.cn (Y. Zhang), Yuanjian.Zhang@seu.edu.cn (Y. Zhang).

protonation/deprotonation process during the conventional thermal condensation [40]. However, the high cost or/and the complicated multiple processes hindered the high synthetic yields and its large-scale applications.

Herein, we report a highly effective and facile way to directly regulate the crystallinity of bulk CN merely by a faster ramping rate in thermal condensation. It was revealed that the promoted condensation kinetics had a profound favorable influence on the crystallinity of the as-prepared bulk CN and the photocatalytic activities as well. No additional chemicals or other complements were needed, the modified condensation recipe was even simpler than the conventional one, but led to an improved photocatalytic H₂ evolution up to 3 times. This work would be promising to greatly pave the large-scale industrial application of bulk CN in sustainable energy, environmental and biosensing applications.

CN was generally synthesized from dicyandiamide (DCDA) by thermal condensation under 550 °C (Fig. 1a) [41]. Previous reports demonstrated that tuning the condensation temperature would introduce more defects and improve the photocatalytic activity [42]. In this study, we argued that the intermediate reactions during the heating process (Fig. 1b) would also affect the final structure of the as-obtained CN. To confirm this hypothesis, different CN was firstly synthesized from DCDA through changing the ramping rate and then holding at 550 °C for 4 h in air atmosphere. The ramping time were 4 h, 2 h, 1 h, 20 min, in which the obtained CN are denoted as CN-4 h-4 h, CN-2 h-4 h, CN-1 h-4 h, and CN-20 min-4 h, respectively.

In the first set of experiments, the crystal structure of CN obtained at the different ramping rates were characterized by X-ray diffraction (XRD) as shown in Fig. 1c. CN-4 h-4 h gave two typical diffraction peaks at around 13.2° and 27.4° with a good agreement with previous reports, which were originated from the in-plane structural packing motif and periodic stacking of layers along the *c*-axis, respectively. The CN-20 min-4 h synthesized by high ramping rate exhibited similar XRD patterns, but the diffraction peak at 27.4° was much sharper and more pronounced. According to the Debye-Scherrer formula, smaller full-width at half maximum (FWHM) indicating larger grain size. For further comparison, the full-width at half maximum (FWHM) and the relative intensity ratio of (100) and (002) peak for the different CNs are summarized and listed in Table S1 (Supporting information). It is noted that by increasing the ramping rate, the resultant CN

showed a much narrowed FWHM of (002) peak and increased relative intensity ratio of peak (002) and peak (100), suggesting an improved stack along the *c*-axis. Other ramping rates, namely increasing temperature from room temperature to 550 °C in 1 h and 2 h, were also investigated. It was found the trend of the higher ramping rate the more narrowed FWHM of (002) peak was not changed (Fig. S1a in Supporting information). Moreover, the different holding time at 550 °C were also studied. As shown in Fig. S1b in Supporting information, the FWHM of (002) peak did not altered as evidently, indicating that compared to engineer the ramping rate, the holding time at 550 °C during the polymerization had a less influence on the polymerization kinetics.

To identify the chemical structure of the obtained different carbon nitrides, Fourier transform infrared (FT-IR) spectra was undertaken (Fig. 1d and Fig. S2 in Supporting information). All samples showed the sharp peak at 807 cm⁻¹, which belonged to the breathing mode of tri-*s*-triazine system; meanwhile the peaks between 1200 and 1700 cm⁻¹, characteristic of C=N and C–N stretching vibration modes, were not changed, which suggested the pristine conjugated structure of CN was preserved. The elemental analysis (Table S1) showed that the C/N atomic ratio and the N content for both CN-4 h-4 h and CN-20 min-4 h were almost same. Besides, the UV-vis spectra of CNs also kept almost identical (Fig. S3 in Supporting information), which indicates that the electronic properties and the light absorb ability of these CNs were similar. Therefore, the different CNs had similar tri-*s*-triazine-based chemical structures and electronic structures, but graphitic crystallinity became higher when increasing the ramping rate.

As rapid ramping rate may result in a quick gas (e.g., NH₃) by-product release, which was supposed to generate higher porosity, the N₂ adsorption-desorption isotherms of obtained CNs were further measured. As shown in Table S1 and Fig. S4 (Supporting information), The Brunauer-Emmett-Teller (BET) surface area of CN-20 min-4 h was calculated to be 17.86 m²/g, which is *ca.* twice of that of CN-4 h-4 h (8.68 m²/g). It confirmed that CN-20 min-4 h with the high ramping rate exhibited higher surface area. The scanning electron microscope (SEM) images were also undertaken to get the morphology information of the CNs (Fig. 2). It was found the as-obtained CNs exhibited similar morphology, *i.e.*, lamellar particles with rough surface, and CN-20 min-4 h exhibit slightly larger particles than that of CN-4 h-4 h from the SEM image.

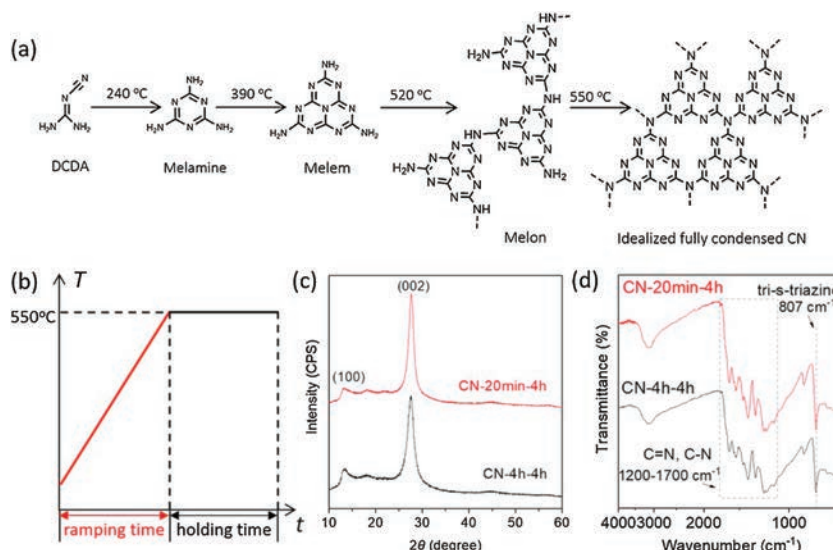


Fig. 1. (a) Scheme of general thermal condensation processes for idealized bulk CN and (b) typical heating programs for bulk CN. (c) XRD patterns and (d) FT-IR spectra of CN-20 min-4 h and CN-4 h-4 h.

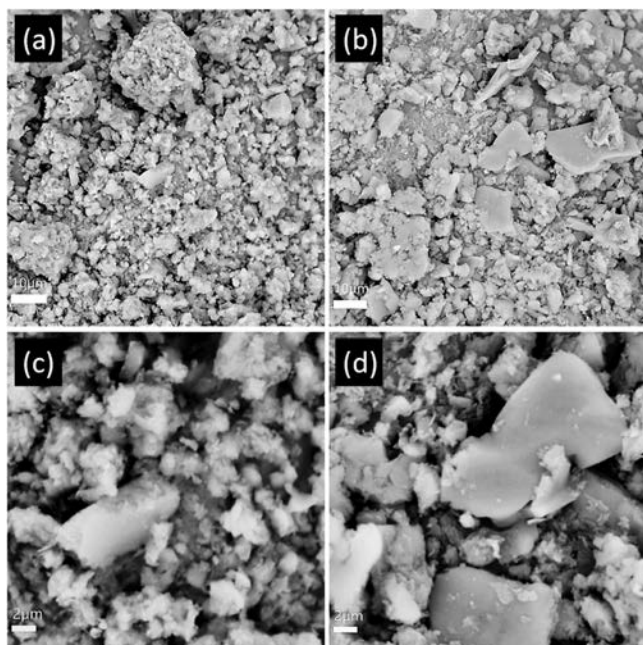


Fig. 2. SEM images of CN-4 h-4 h (a, c) and CN-20 min-4 h (b, d).

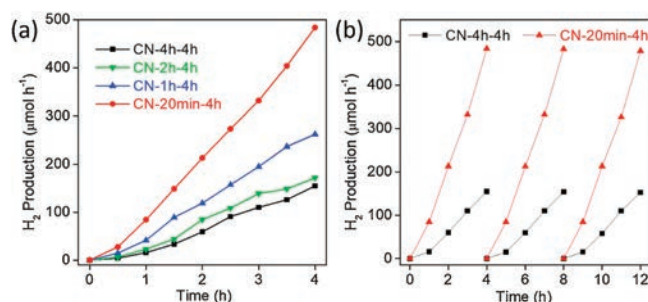


Fig. 3. (a) The photocatalytic H₂ evolution rate of CN-x-4 h (x = 20 min, 1 h, 2 h, 4 h), and (b) the photocatalytic stability test of CN-20 min-4 h and CN-4 h-4 h.

However, the BET surface area of them demonstrated more evident changes. To understand the contribution from pores of different size, the cumulative pore volume was calculated from the desorption branches of N₂ adsorption-desorption isotherms using Barret-Joyner-Halender (BJH) method. As shown in Fig. S4b, the pore volume of CN-20 min-4 h was higher than CN-4 h-4 h, demonstrated more pore structure in the material. It could be presumably due to the quick gas release during the fast ramping process.

The photocatalytic activities of the obtained CNs were also evaluated by H₂ evolution under visible light irradiation ($\lambda > 420$ nm) with a Pt nanoparticle co-catalyst as the electron traps and hydrogen evolution sites. Fig. 3a illustrated that the average hydrogen evolution rate of the CN-20 min-4 h reached 121.0 $\mu\text{mol h}^{-1} \text{g}^{-1}$, which was almost 3 times higher than that of the CN-4 h-4 h (38.7 $\mu\text{mol h}^{-1} \text{g}^{-1}$). Compared with previous reported methods for higher crystallinity (Table S2), this work exhibited a favorable photocatalytic performance, especially no additional chemicals were needed in synthesis process. It was noting that the H₂ generation capability of CNs increased along with the raise of ramping rate. Moreover, no noticeable deactivation was observed even after three cycles of hydrogen evolution tests (Fig. 3b), implying that as-prepared CNs had excellent photocatalytic stability. Besides, the photocatalytic activities of CNs synthesized by different holding time at 550 °C were also explored, but no apparent changes were observed (Fig. S5 in Supporting information). Therefore, the larger specific surface area of CN-20 min-4 h and the crystallinity improvement from rapid ramping rate were supposed to be primarily account for the enhanced photocatalytic performances.

To further understand the mechanism of improved photocatalytic activity of CNs, the separation and recombination behavior of the photogenerated charge carriers were studied by photoelectrochemical test and photoluminescence (PL) spectra. The photochemical activities of all as-prepared CN were evaluated by photocurrent generation in a standard photoelectrochemical cell (PEC) configuration under visible light irradiation. As shown in Fig. 4a, CN of higher ramping rate exhibited more evident photocurrent under all biased potential. It was further confirmed in Fig. 4b that CN-20 min-4 h showed the highest cathode transient current response (biased at -0.2 V), and was about 2 times larger than that of conventional CN-4 h-4 h. The photocurrent enhancement indicates the improved separation of photo-induced electron-hole pairs, which was an essential step for the photocatalytic hydrogen evolution process [43]. Moreover, PL spectra of CNs were obtained with an excitation wavelength of 350 nm at room temperature. As shown in Fig. 4c, CN-20 min-4 h showed a lower fluorescence intensity than CN-4 h-4 h, implying the suppressing of energy-wasteful charge recombination and promoting the charge separation, which may offer more opportunities for excited electrons or holes to participate in the photocatalytic reaction [14]. Thus, different to previous works of improving photocatalytic performance by modulating the polymerization temperature, simply engineering of the heating ramping rate significantly altered the crystallinity and surface area of CNs, which was beneficial to the separation efficiency of charge carriers, leading to the tremendously improved photocatalytic activity.

In summary, we have developed a facile method to prepare CN with improved surface area and crystallinity merely by increasing the ramping rate. Compared to the general synthesized bulk CN, CN

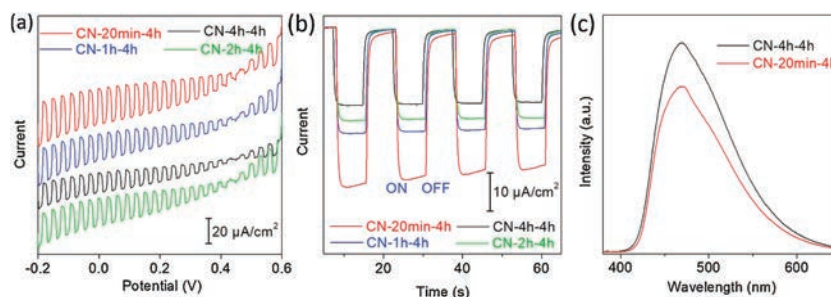


Fig. 4. (a) I-V curve and (b) the transient current response of CN-x-4 h (x = 20 min, 1 h, 2 h, 4 h) biased at -0.2 V in 0.1 mol/L KCl under irradiation of chopped visible light ($\lambda > 420$ nm). (c) The PL spectra of CN-20 min-4 h and CN-4 h-4 h under 350 nm excitation.

obtained from fast ramping rate demonstrated higher charge separation efficiency as a result of higher crystallinity, larger surface area by quick gas release during the condensation process. Therefore, the photocurrent and photocatalytic hydrogen production were enhanced strikingly. This work by optimization of the thermal condensation kinetics provide an even more facile method with respect to the common condensation recipe to prepare bulk CN with additional beneficial in boosting the photocatalytic activities of bulk CN without any use of template and chemical doping. Therefore, it is highly envisaged that this method could be easily expanded to manufacture of bulk CN for potential large-scale industrial applications with enhanced photocatalytic activities in water splitting, photocatalytic degradation of organic pollutants, and optical biosensing.

Acknowledgments

This work was financially supported in part by the National Natural Science Foundation of China (Nos. 21775018, 21675022), the Natural Science Foundation of Jiangsu Province (Nos. BK20160028, BK20170084), the Postgraduate Research & Innovation Program of Jiangsu Province (No. KYCX17_0137), the Open Funds of the State Key Laboratory of Electroanalytical Chemistry (No. SKLEAC201909) and the Fundamental Research Funds for the Central Universities.

Appendix A. Supplementary data

Supplementary material related to this article can be found, in the online version, at doi:<https://doi.org/10.1016/j.ccl.2019.04.068>.

References

- [1] R. Asahi, T. Morikawa, T. Ohwaki, et al., *Science* 293 (2001) 269–271.
- [2] Y.F. Xu, M.Z. Yang, B.X. Chen, et al., *J. Am. Chem. Soc.* 139 (2017) 5660–5663.
- [3] A. Fujishima, K. Honda, *Nature* 238 (1972) 37–38.
- [4] X.B. Chen, L. Liu, P.Y. Yu, et al., *Science* 331 (2011) 746–750.
- [5] A. Naseri, M. Samadi, A. Pourjavadi, et al., *J. Mater. Chem. A* 5 (2017) 23406–23433.
- [6] L. Zhou, Y.F. Xu, B.X. Chen, et al., *Small* 14 (2018) 1703762.
- [7] X. Wang, K. Maeda, A. Thomas, et al., *Nat. Mater.* 8 (2009) 76–80.
- [8] Y. Wang, X. Wang, M. Antonietti, *Angew. Chem. Int. Ed.* 51 (2012) 68–89.
- [9] Y. Zhang, T. Mori, J. Ye, *Sci. Adv. Mater.* 4 (2012) 282–291.
- [10] G. Liu, T. Wang, H. Zhang, et al., *Angew. Chem. Int. Ed.* 54 (2015) 13561–13565.
- [11] Y. Zheng, L. Lin, B. Wang, et al., *Angew. Chem. Int. Ed.* 54 (2015) 12868–12884.
- [12] W.J. Ong, L.L. Tan, Y.H. Ng, et al., *Chem. Rev.* 116 (2016) 7159–7329.
- [13] K. Schwinghammer, B. Tuffly, M.B. Mesch, et al., *Angew. Chem. Int. Ed.* 52 (2013) 2435–2439.
- [14] Q. Han, B. Wang, Y. Zhao, et al., *Angew. Chem. Int. Ed.* 54 (2015) 11433–11437.
- [15] J. Liu, Y. Liu, N. Liu, et al., *Science* 347 (2015) 970–974.
- [16] H. Shi, G. Chen, C. Zhang, et al., *ACS Catal.* 4 (2014) 3637–3643.
- [17] L. Shi, T. Wang, H.B. Zhang, et al., *Adv. Funct. Mater.* 25 (2015) 5360–5367.
- [18] H.J. Feng, Q.Q. Guo, Y.F. Xu, et al., *Chemoschem* 11 (2018) 4256–4261.
- [19] S.C. Yan, Z.S. Li, Z.G. Zou, *Langmuir* 25 (2009) 10397–10401.
- [20] J.Y. Su, L. Zhu, P. Geng, et al., *J. Hazard. Mater.* 316 (2016) 159–168.
- [21] T.Y. Ma, Y.H. Tang, S. Dai, et al., *Small* 10 (2014) 2382–2389.
- [22] Y.Q. Lv, S.Y. Chen, Y.F. Shen, et al., *J. Am. Chem. Soc.* 140 (2018) 2801–2804.
- [23] K. Patir, S.K. Gogoi, *ACS Sustain. Chem. Eng.* 6 (2018) 1732–1743.
- [24] P. Niu, L. Zhang, G. Liu, et al., *Adv. Funct. Mater.* 22 (2012) 4763–4770.
- [25] D.J. Martin, K. Qiu, S.A. Shevlin, et al., *Angew. Chem. Int. Ed.* 53 (2014) 9240–9245.
- [26] S. Cao, J. Low, J. Yu, et al., *Adv. Mater.* 27 (2015) 2150–2176.
- [27] H. Yu, R. Shi, Y. Zhao, et al., *Adv. Mater.* 29 (2017) 1605148.
- [28] Z.X. Zhou, Y.Y. Zhang, Y.F. Shen, et al., *Chem. Soc. Rev.* 47 (2018) 2298–2321.
- [29] G. Liu, P. Niu, C. Sun, et al., *J. Am. Chem. Soc.* 132 (2010) 11642–11648.
- [30] K. Wang, Q. Li, B.S. Liu, et al., *Appl. Catal. B-Environ* 176 (2015) 44–52.
- [31] F. Goettmann, A. Fischer, M. Antonietti, et al., *Angew. Chem. Int. Ed.* 45 (2006) 4467–4471.
- [32] J.H. Wang, C. Zhang, Y.F. Shen, et al., *J. Mater. Chem. A* 3 (2015) 5126–5131.
- [33] Y.F. Shen, C. Zhang, C.G. Yan, et al., *Chin. Chem. Lett.* 28 (2017) 1312–1317.
- [34] M.Y. Ye, Z.H. Zhao, Z.F. Hu, et al., *Angew. Chem. Int. Ed.* 56 (2017) 8407–8411.
- [35] Y.L. Chen, Z.S. Zhan, J.H. Wang, et al., *Chin. Chem. Lett.* 29 (2018) 437–440.
- [36] Z.Z. Kong, X.Z. Chen, W.J. Ong, et al., *Appl. Surf. Sci.* 463 (2019) 1148–1153.
- [37] M. Shalom, S. Inal, C. Fettkenhauer, et al., *J. Am. Chem. Soc.* 135 (2013) 7118–7121.
- [38] X.H. Li, J.S. Zhang, X.F. Chen, et al., *Chem. Mater.* 23 (2011) 4344–4348.
- [39] Y.F. Guo, J. Li, Y.P. Yuan, et al., *Angew. Chem. Int. Ed.* 55 (2016) 14693–14697.
- [40] J.H. Wang, Y.F. Shen, Y. Li, et al., *Chem. -Eur. J.* 22 (2016) 12449–12454.
- [41] A. Thomas, A. Fischer, F. Goettmann, et al., *J. Mater. Chem.* 18 (2008) 4893–4908.
- [42] V.W.H. Lau, M.B. Mesch, V. Duppel, et al., *J. Am. Chem. Soc.* 137 (2015) 1064–1072.
- [43] J.H. Wang, Y.L. Chen, Y.F. Shen, et al., *Chem. Commun.* 53 (2017) 2978–2981.